Journal of Operation and Automation in Power Engineering

vol. XX, no. XX, Dec. 2022, Pages: XXXX (Proofed)

http://joape.uma.ac.ir

Empirical Mode Decomposition and Optimization Assisted ANN Based Fault Classification Schemes for Series Capacitor Compensated Transmission Line

O. Koduri[1,], R. Ramachandran[1], M. Saiveerraju[2]*

[1] *Department of Electrical Engineering, Faculty of Engineering & Technology, Annamalai University, Annamalainagar, 608002, Tamil Nadu, India.*

[2] *Department of Electrical & Electronics Engineering, Sagi Rama Krishnam Raju Engineering College Bhimavaram-534202, Andhra Pradesh, India*

Abstract— *This paper presents two intelligent classifier schemes for classifying the faults in a series capacitor compensated transmission line (SCCTL). The first proposed intelligent classifier scheme is a particle swarm optimization-assisted artificial neural network (PSO-ANN). The second, proposed one is a teaching-learning optimization-assisted artificial neural network (TLBO-ANN). For each type of fault, the 3-phase current signals are acquired at the sending end and processed through empirical mode decomposition (EMD), to decompose into six intrinsic mode functions. The neighborhood component analysis is used to extract the best feature intrinsic mode functions. From the identified best feature intrinsic mode functions, the energy of each phase of the line is computed. The energy of each phase is fed as inputs for both PSO-ANN and TLBO-ANN classifiers. The practicability of the proposed intelligent classifier schemes has been tested on a 500 kV, 50 Hz, and 300 km long line with a midpoint series capacitor using MATLAB/Simulink Software. The results demonstrate that the classifier schemes are able to accurately classify faults in less than a half-cycle. Furthermore, the efficacy of the proposed intelligent classifier schemes has been evaluated using Performance Indices including Kappa Statistics, Mean Absolute Error, Root Mean Square Error, Precision, Recall, F-measure, and Receiver Operating Characteristics. From the results of Performance Indices, it is concluded that the proposed TLBO-based artificial neural network classifier outperforms the PSO-based artificial neural network classifier. Finally, the efficacies of proposed intelligent classifier schemes are compared to existing approaches.*

Keywords—Artificial Intelligence: Particle swarm optimization-assisted artificial neural network, Teaching-learning-optimization-assisted artificial neural network, Power System Faults: Identification, Series capacitor compensation line, Signal Processing: Empirical mode decomposition.

NOMENCLATURE

KV	Kilo Volts
Km	Kilo meter
Hz	System frequency
$X(t)$	Input signal
n_1	Mean of the signal
$m(t)$	Number of IMFs
$r(t)$	Residue
v_k	Velocity of the particle
p_k	Position of the particle
$p_{k\,best}$	Best position of particle at k^{th} instant
g_{best}	Global best
W	Controlling parameter
S_1 and S_2	Arbitrary variables
c_1 and c_2	Weights control parameters
PSO	Particle Swarm Optimization
ANN	Artificial Neural Network
TLBO	Teaching Learning Based Optimization
m	No of subjects
n	No of learners
T_F	Teaching factor
$Y_{total-pbest}$	Teaching Best overall result
E_p	Predicted samples
E_o	Observed samples
T_p	True Positive samples
F_p	False Positive samples
F_N	False Negative samples
P	Precision
R	Recall
IMFs	Intrinsic mode functions
E_A	Energy of Phase A
E_B	Energy of Phase B
E_C	Energy of Phase C
MSE	Mean square error
y_{kl}	Target output
Y_{kl}	Actual output
N	No of samples

Received: 23 Jan. 2023
Revised: 28 Apr. 2023
Accepted: 01 Jun. 2023
*Corresponding author:
E-mail: kodurieee@gmail.com (O. Koduri)
DOI: 10.22098/joape.2023.12112.1899
Research Paper

1. INTRODUCTION

1.1. Motivation and incitement

Nowadays, the electricity load demand continually increases across many regions of the world. The existing long transmission

corridor capacity is scarce to meet the increased load demand due to the thermal stability limit. The fixed series capacitor compensated long line is considered a suitable solution to optimize the transmission assets. Moreover, the advantages of fixed series capacitor compensation lines improve the power transfer capability and increase the system stability. However, due to the nonlinear behavior of the series capacitor, the distance measurement changes suddenly for a particular type of line faults, and it will affect the relay functionality [1]. Conventional distance protection is a challenging task as the variation of the impedance seen by the relay is different from fault location before and after the series capacitor [1, 2]. In [2], incorporating a series capacitor in the transmission line introduces different challenges and problems, including distance reach problems and directional discrimination issues for distance relays. For the protection of transmission systems, a model-based approach such an adaptive Kalman filtering scheme was previously recommended. A Kalman filter design was necessary for such a protection strategy, however because of the chosen linear model, the filter may rapidly diverge if the initial estimate of the state is off or the process is poorly described. There have been numerous attempts to classify faults using a travelling wave-based methodology in the past. However, the travelling wave approach [3] requires a high sample rate and has trouble distinguishing between waves reflected from the fault and those from the distant end of the line. Fuzzy logic was used to categorise the problems in relaying fault classifications [4]. The benefit of fuzzy logic is that it uses simple "IF- THEN" relationships to directly convey information. However, logic-based expert systems encounter the combinatorial explosion problem when applied to large systems [4]. Again, the correctness of fuzzy logic-based approaches cannot be guaranteed for highly variable system parameters. Girgis and Johns [5] used a phasor measurement unit (PMU)-based technique that was created in [6] for fault analysis. These techniques have the drawback of requiring phasor calculation. Artificial neural networks (ANNs) have gained a lot of attention over the past two decades due to their computational speed and robustness in fields such as pattern classification, digital signal processing, intelligent control, power system analysis, fault detection and classification, data compression, analysis for solving power quality problems, power quality assessment, protection, transient analysis, and others [7]. Even though there are many different neural network architectures, only a few of them are used in industry. Back-propagation neural network (BPNN), the most popular type of neural network design, is built on a multi-layer perceptron and use supervised learning to uncover complex, nonlinear, multidimensional mathematical fits. The fault classification with high-quality accuracy in less time is challenging. For accurate estimation of fault location, the classification of faults is necessary, and this information is essential for protection engineers to take up action against the quick repair and maintenance work and restoration of lines to improve the system's reliability.

1.2. Literature Review

1) Commercial Approaches:

Phase angle between sequence current and voltage based approach are generally utilized in commercially available relays for fault type classification [8, 9]. The relay compares the relative angles between pure-fault sequence currents available at the local end and identifies the fault type in the network [8]. This approach is effected by fault location and fault inception angle. Some relays utilized the angle difference between negative and zero sequence current only in [9], by avoiding adverse effect of positive sequence phase angle variation. But this approach is effect by fault resistance and fault location and fault inception angle variations.

2) Data Driven Approaches with /without Signal Processing Tools:

The protective relaying algorithms based on computational intelligence are recommended for uncompensated lines in [10]. The magnitude of differential power feature-based decision tree protection scheme for fault classification with a proper threshold has been suggested for an uncompensated transmission line in [11]. In [12], wavelet analysis and statistical feature-based hybrid PSO-ANN classifiers are reported. However, the scheme's drawback is to evaluate the two-stage algorithm, and hence the complexity burden increases. In [13], the empirical mode decomposition-based SVM model was introduced for fault classification of the uncompensated line. However, this classifier scheme provides less acceptable percentage accuracy. In [14], the empirical mode decomposition-based artificial neural network has been proposed in uncompensated transmission lines for fault diagnosis. Nevertheless, this protection scheme requires an extensive data set to train the network, leading to a computational burden. The wavelet transform-based chebyshev neural network was introduced in [15] for classifying the faults. In [16], the intelligent classifier scheme is reported for fault classification. Nevertheless, the intelligent classifier model is complex, and it provides less accuracy. The Chebyshev Neural Network based inter fault classifier is reported in [17]. However, the drawback of this method requires the large training and testing data need for classification. The data mining based Support vector machine fault classification for micro grid is implemented in [18]. The advantage of this method is it obtained the high accuracy with less time. The intelligent model to forecast market clearing price using a multilayer perceptron neural network, based on structural and weights optimization is presented in [19]. The merits of this model is its obtained high classification accuracy. In [20], the extreme learning machine based fault detection and classification for transmission line is implemented. The advantage of this method is shorter processing time and reduced computational complexity. Fault classification of transmission line using different machine learning techniques are reported in [21]. Teager Kaiser energy operator (TKEO) and extreme gradient boost (XGBoost) based fault detection and classification in transmission line is implemented in [22]. In [23], the multi-dimensional aggregation and decoupling network (MADN) is proposed. However, this method needs the large data set for training/testing leading to computational burden. Transfer learning approach for fault classification in transmission line is implemented in [24].

According to the literature review, the fault classification is categorized as the commercial approaches and data driven with/without signal processing approaches. In data driven with signal processing approaches most of the research studies have been presumed to classify the uncompensated and series-compensated line faults. Compared to the uncompensated line, fault classification is challenging for series-compensation lines due to the existence of a series capacitor. The quick identification of faults is necessary for maintain the security and reliability of the system. In this connection, the fault classification study is essential for series compensated lines.

In this article the Empirical Mode Decomposition and optimization assisted ANN based Fault classification schemes for series capacitor compensated transmission line is proposed. The Empirical mode decomposition signal processing method is used for feature extraction. The advantage of this method is it is adaptive and applicable to non-stationary signals (Fault signals) and swarm intelligence and metaheuristic based optimization ANN methods are used to get the better accuracy. Finally, the proposed EMD based PSO-ANN and TLBO-ANN classifiers are robust to fault resistance, fault location, fault inception and load variations etc.

The critical contribution of proposed optimization-assisted intelligent classifier schemes is summarized as follows

- A framework based on combination of empirical mode decomposition and optimization assisted two intelligent classifier schemes (PSO-ANN and TLBO-ANN) are proposed

to classify the faults.
- Features extracted from the empirical mode decomposition and neighborhood component analysis algorithm is used to train and test the proposed two classifier schemes.
- Proposed PSO-ANN and TLBO-ANN classifier schemes achieve an accuracy of 99.92% and 99.98%, respectively, with high speed and reduced memory.
- Performance indices were used to validate the proposed two intelligent classifier schemes.

The structure of this manuscript is presented and, starting with section 2, which deals with the description of the system studied & methodology. As an extension, the empirical mode decomposition technique is discussed clearly in section 3. Section 4 deliberates the theoretical framework of the proposed intelligent classifier schemes and performance indices. Section 5 presents the empirical mode decomposition, neighbourhood component analysis based feature extraction, and simulation of proposed intelligent classifier schemes. Section 6, simulation results, discussions of proposed intelligent classifier schemes, and performance analysis are presented. The evaluation of case studies and comparative assessment with different existing methods along with critical conclusions are placed in section 7 & section 8 respectively.

2. System Analysis and Methodology

To validate the proposed two classifier schemes, all types of fault simulations are performed using MATLAB/Simulink software as shown in Fig. 1, with a significant system operating conditions.

2.1. Series Capacitor Compensation Line with Proposed Intelligent Classifier Schemes

Fig.1 shows that, schematic single line diagram of $500\,kV$, $50\,Hz$, and $300\,km$ long series capacitor compensated line with sources at each ends. Bus1 and Bus2 are linked with the 300 long line and compensated with a 40 % compensation factor by the series capacitor. A sampling frequency of $8\,kHz$ is chosen for simulation studies. The parameters for the system are given in Appendix A.

As shown in Fig. 11, the steps for the EMD based optimization assisted proposed intelligent fault classifier schemes are as follows.
Step1: Pre-processing:
For collecting fault current data, the various symmetrical and unsymmetrical fault scenarios are considered on series capacitor compensated line.
Step-2: Advanced signal processing technique:
The fault current signals are passed through EMD and extracted into six intrinsic mode functions (IMFs).
Step-3: Neighborhood component analysis based best feature extraction:
The NCA algorithm is used to identify the best feature IMFs from the identified six intrinsic mode functions.
Step-4: Calculation of each phase energy:
The obtained best feature IMFs are used to calculate the phase energy(s) E_A, E_B, and E_C.
Step-5: Training phase:
The proposed two intelligent classifiers, PSO-ANN and TLBO-ANN, are trained using the data obtained (E_A, E_B, and E_C) from EMD and NCA under various symmetrical and unsymmetrical fault scenarios.
Step-6: Fault type:
The output of the proposed classifier schemes provides the classification of symmetrical and unsymmetrical types of faults.

3. Empirical Mode Decomposition (EMD) Analysis

Empirical mode decomposition (EMD) [25], is a modern and robust method for analyzing non-linear and non-stationary signals. Unlike wavelet transform, EMD has a self-adaptive signal processing technique. EMD executes the operation that separates a series into IMFs without ignoring the time domain. According to [10], an EMD decomposes the signal into the corresponding IMFs through the sifting process. According to [6], an IMF is any function whose envelopes is symmetrical concerning zero, with the same number of extreme and zeros crossings.

The decomposition of the measured input signal $X(t)$ by EMD is described as follows.

1. The measured signal $X(t)$ identifies the local maxima and minima and interpolates the extreme points to obtain upper and lower envelopes from cubic splines.
2. The n_1 represent the mean of $X(t)$ upper and lower envelops.
3. CalculateS_1using Eq. (1)

$$S_1 = X(t) - n_1 \tag{1}$$

4. In this step theS_{11} is obtained as, the subtraction of S_1 from then_{11}, and is expressed as Eq. (2)

$$S_{11} = S_1 - n_{11} \tag{2}$$

Here n_{11} represent the mean of S_1 signal upper and lower envelops.
5. The above process is repeated j times, until S_{1j} satisfies the IMF situation. Then, it is chosen as the first IMF. $b_1 = S_{1j}$, The first IMF is subtracted from the input signal.
Then, calculate

$$R_1 = X(t) - b_1 \tag{3}$$

6. R_1 is chosen as the main signal and repeats the steps 1–5.
7. In this step, the above process is repeated until the R_n becomes monotonic.
8. Finally, the measured signal is decomposed into m number of IMFs and a residue $r(t)$, as expressed in Eq. (4).

$$y(t) = \sum_{j=1}^{m} m(t) + r(t) \tag{4}$$

The IMFs are extracted from current signals and condition is satisfied, then check with residue is monotonic, if it is yes process is terminated: the entire procedure [13], is represented in Fig. 2.

4. Theoretical Framework of Proposed Intelligent Classifier Schemes

4.1. PSO-ANN classifier scheme

A) Particle swarm optimization

The Back Propagation Neural Network (BPNN) method is the most widely used neural network for solving nonlinear problems, yet the early BP networks used to suffer mostly from slower convergence because they used to become stuck at local minima. The convergence behaviour is depends on initial weights, learning rate and momentum. To overcome the above draw back swarm intelligence algorithm is proposed.

The PSO is a population-based stochastic optimization algorithm [26] that takes its inspiration from the intelligent group behaviour of fish schools and bird flocks. This algorithm is a computational technique and has many similarities with evolution algorithms. The PSO is computationally superior compared to evolution algorithms in terms of computer memory space and speed specifications.

Computational procedure of PSO-algorithm as follows [10].
Step1: Initialization Process
All particle velocity and position are arbitrarily initialized within the pre-specified range.
Step 2: Velocity Updating Process
All particle velocities are updated with the following rule.

$$v_k^r(t+1) = w \cdot v_k^r(t) + c_1 \cdot S_1 \cdot (\overrightarrow{p_{k,best}} - x(t)) + c_2 \cdot S_2 \cdot (\overrightarrow{g_{best}} - x(t))$$
$$x(t+1) = x(t) + v_k^r(t+1) \tag{5}$$

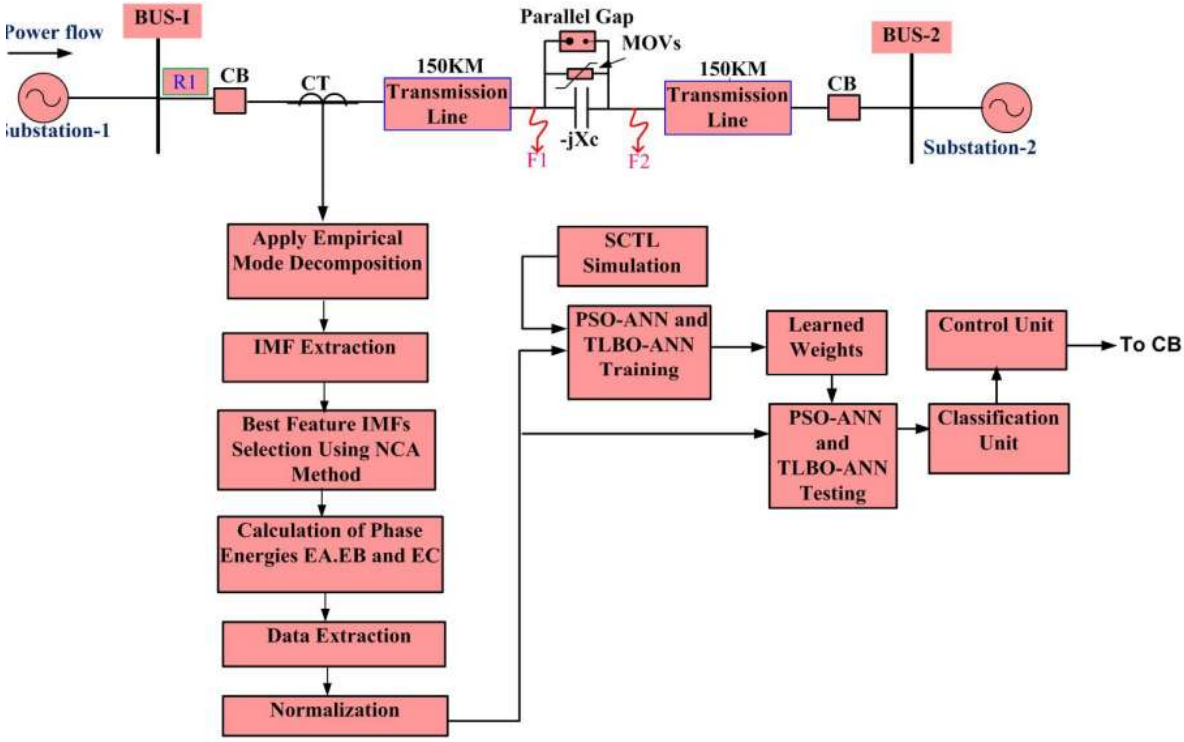

Fig. 1. Schematic diagram of proposed EMD based intelligent fault classifier schemes

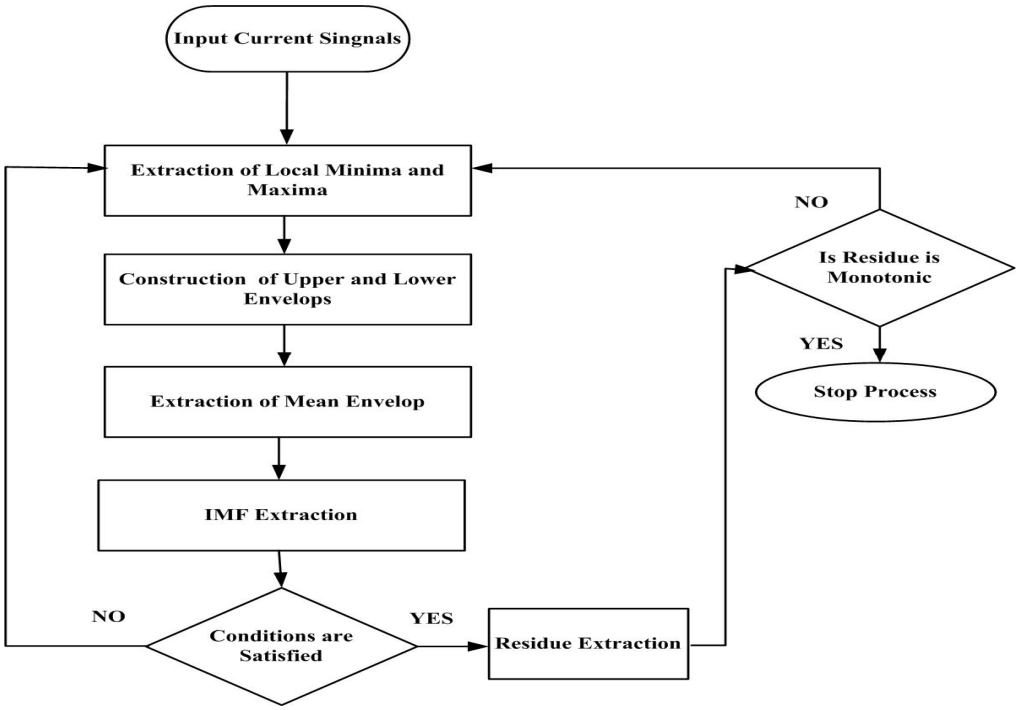

Fig. 2. Flow diagram for empirical mode decomposition process

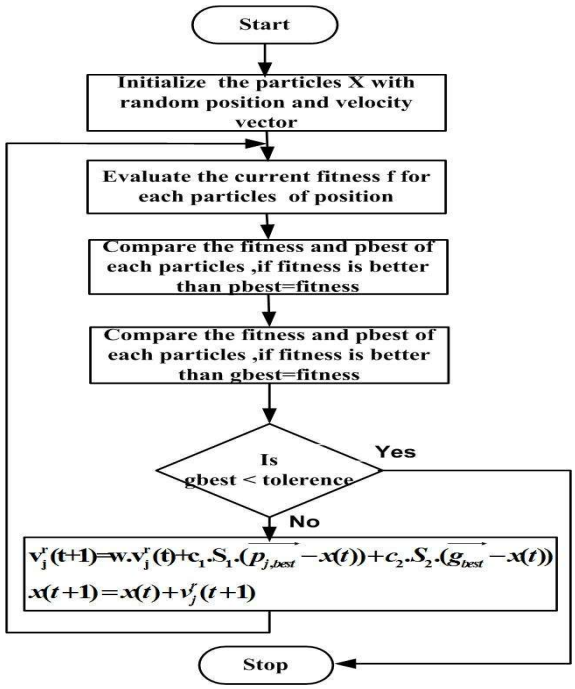

Fig. 3. Flow chart for PSO-Algorithm

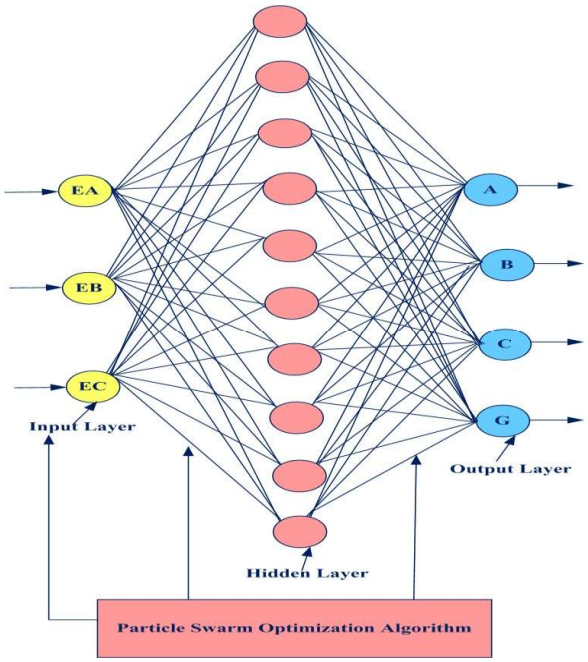

Fig. 4. Architecture for PSO-ANN classifier

where v_k^r and p_k are the velocity and position of the k^{th} particle.

$\overrightarrow{p_{k,best}}$ is the position of particle at k^{th} instant best object value for one population.

$\overrightarrow{g_{best}}$ is the position of a particle with the best global object for the entire population.

w is the controlling parameter of the flying bird.

S_1 and S_2 are the arbitrary variable with range [0,1].

c_1 and c_2 are weights control parameters.

Step 3: Position Updating Process

According to the following rule, all particle positions are updated.

$$\overrightarrow{p_k} \leftarrow \overrightarrow{p_k} + \overrightarrow{v_k} \tag{6}$$

Step 4: Memory Updating Process

According to the following rule the $\overrightarrow{p_{k,best}}$ and $\overrightarrow{g_{best}}$ are updated.

$$\overrightarrow{p_{k,best}} \leftarrow \overrightarrow{p_k} if(\overrightarrow{p_k}) \succ f(\overrightarrow{p_{k,best}}), \overrightarrow{g_{best}} \leftarrow \overrightarrow{p_k} \text{ if } (\overrightarrow{p_k}) \succ f(\overrightarrow{g_{best}}) \tag{7}$$

$$v_k^r(t+1) = w \cdot v_k^r(t) + c_1 \cdot S_1 \cdot (\overrightarrow{p_{k,best}} - x(t)) + c_2 \cdot S_2 \cdot (\overrightarrow{g_{best}} - x(t))$$
$$x(t+1) = x(t) + v_k^r(t+1) \tag{8}$$

Step 5: Checking procedure for termination.

The above process steps 2–4 are repeated until the annihilation condition is met. Finally, the solution reports as the $\overrightarrow{g_{best}}$ and $f(\overrightarrow{g_{best}})$

The computation process of the particle swarm optimization technique is represented in followed flow chart.

4.2. PSO-ANN algorithm

In this work, the three-layered, three inputs and four outputs feed-forward (i.e., MLP) [27], ANN with particle swarm optimization assisted algorithm is considered for fault classification. In this study, the ten numbers neurons are selected in the hidden layer using the trial and error approach. It should give the best performance. Therefore, the total numbers of weights presented in architecture are $3 \times 10 + 10 \times 4 = 70$ weights. For better accuracy of the proposed classifier is obtained by the network weights are optimized through the PSO algorithm.

For the PSO-ANN classifier scheme, the output value is 1 indicates the fault phase, and the value is 0 indicates the healthy phase, as shown in Fig. 4.

4.3. TLBO-ANN classifier scheme

A) TLBO Algorithm

The algorithm specific parameters are required for all the swarm intelligence and evolutionary-based algorithms. Improper selection and tuning of the algorithm-specific control parameters leads to the local optimal solution, which is a significant factor influencing the efficiency of the algorithm. The implementation of TLBO algorithm is more easily because no tuning of algorithm-specific parameters is needed [28]. To overcome the Back propagation algorithm and PSO algorithm draw back, the meta- heuristics such as TLBO algorithm is proposed.

B) Steps for TLBO Algorithm

1. Teacher Stage

Consider 'm' number of subjects, 'n' number of learners (i.e, population size $k = 1, 2, \ldots, n$) and the

$N_{j,i}$ be the mean result of the learners in a particular subject 'j'$(j = 1, 2, \ldots, m)$.

The best overall result is $Y_{total-p_{best\,i}}$.
The difference mean is calculated by using Eq. (9).

$$\text{Difference\_mean}_{j,k,i} = r_i(Y_{j-p_{best,i}} - T_F N_{j,i}) \quad (9)$$

where, $Y_{j-p_{best,i}}$ is the result of the best learner in subject j.
T_F is the teaching factor, and r_i is random number between [0, 1].
The T_F is either 1 or 2.
The T_F is obtained from the Eq. (10).

$$T_F = round[1 + rand(0,1)\{2-1\}] \quad (10)$$

The existing solution is updated in teacher phase according to Eq. (11).

$$Y'_{j,k,i} = Y_{j,k,i} + \text{Difference\_mean}_{j,k,i} \quad (11)$$

In this phase the updated value $Y'_{j,k,i}$ is accepted then it gives the enhanced function value.

2. Learner Stage

The learner communicates with other learner spontaneously during this process, a learner, while other learner has more experience, learn new things. Selecting a population size of 'm', the occurrence of the learning for this stage is explained below.
Choose randomly R and$S$ learners.
Such that $Y'_{total-R,k} \neq Y_{total-S,k}$ (where, $Y'_{total-R,k}$ and $Y'_{total-S,k}$ are the simplified function values of $Y_{total-R,k}$ and $Y_{total-S,k}$ of R and S respectively at the end of teacher phase.

$$Y''_{l,R,k} = Y'_{l,R,k} + r_i(Y'_{l,R,k} - Y^i_{l,S,k}) \text{ if } Y'_{total-R,k} \prec Y'_{total-S,k} \quad (12)$$

$$Y''_{l,R,k} = Y'_{l,S,k} + r_k(Y'_{l,R,k} - Y^i_{l,S,k}) \text{ if } Y'_{total-R,k} \prec Y'_{total-S,k} \quad (13)$$

The $Y'_{l,R,k}$ is accepted, if it gives a better function value.

The computation process of the teaching-learning optimization algorithm is illustrated as shown in Fig. 5.

4.4. TLBO ANN Algorithms

In this work, the three-layered, three inputs and four outputs feed-forward (i.e., MLP) [27], ANN with teaching learning-based optimization-assisted algorithm is selected as shown in Fig. 6. In this study process, the ten numbers of neurons are selected in the hidden layer by trial and error approach. It should give the best performance. Therefore, the total numbers of weights presented in architecture are $3 \times 10 + 10 \times 4 = 70$ weights. To obtain the better accuracy of the proposed classifier, by optimizing the network weights through the TLBO algorithm.

For the TLBO-ANN classifier scheme, the output value is 1 indicates the fault phase, and the value is 0 indicates the healthy phase, as shown in Fig. 6.

4.5. Performance indices

A) Kappa Statistics (KS)

It is used to calculate the accuracy of expected and observed data sets and is expressed by Eq. (14).

$$K = \frac{P(OF) - P(EF)}{1 - P(EF)} \quad (14)$$

where $P(OF)$ is the probability that a system would experience an observed fault, whereas $P(EF)$ is the probability that a predicted fault may inadvertently occur in the system [29].

B) Mean absolute error (MAE) and Root mean square error (RMSE)

It is defined as the difference between the predicted and observed samples of a classifier [29].

$$MAE = \frac{|\sum_{i=1}^{n}(E_P - E_O)|}{n} \quad (15)$$

RMSE is the average deviations of the predications from the observations, and it is given by

$$RMSE = \sqrt{\frac{\sum_{i=1}^{n}(E_P - E_O)^2}{n}} \quad (16)$$

where E_O is the observed and E_P is the predicted samples.

C) Precision (P)

It is ratio of true positive samples to the sum of true positive and false positive samples [29].

$$Precision = \frac{T_P}{T_P + F_P} \quad (17)$$

D) Recall (R)

It is a ratio of the true positive samples divided by the total number of true positive and false negative samples [29].

$$Recall = \frac{T_P}{T_P + F_N} \quad (18)$$

E) F-measure

It is ratio of twice the product of precision and recall to the sum of precision and recall [29],

$$F - Measure = \frac{(2 \times P \times R)}{P + R} \quad (19)$$

F) Receiver Operating Characteristic (ROC)

The area under the ROC curve represents the classification capability of the algorithm, it approaches to one, indicates that the classification prediction was the most precise and accurate [29].

5. Empirical Mode Decomposition, Neighbourhood Component Analysis Based Feature Extraction and Simulation of Proposed Intelligent Classifier Schemes

5.1. Pre-processing of current signals through Empirical Mode Decomposition and IMF extraction

The three-phase line current signals, I_a, I_b, and I_c are measured at the sending end of the SCCTL line. These current waveforms during normal and AG fault conditions

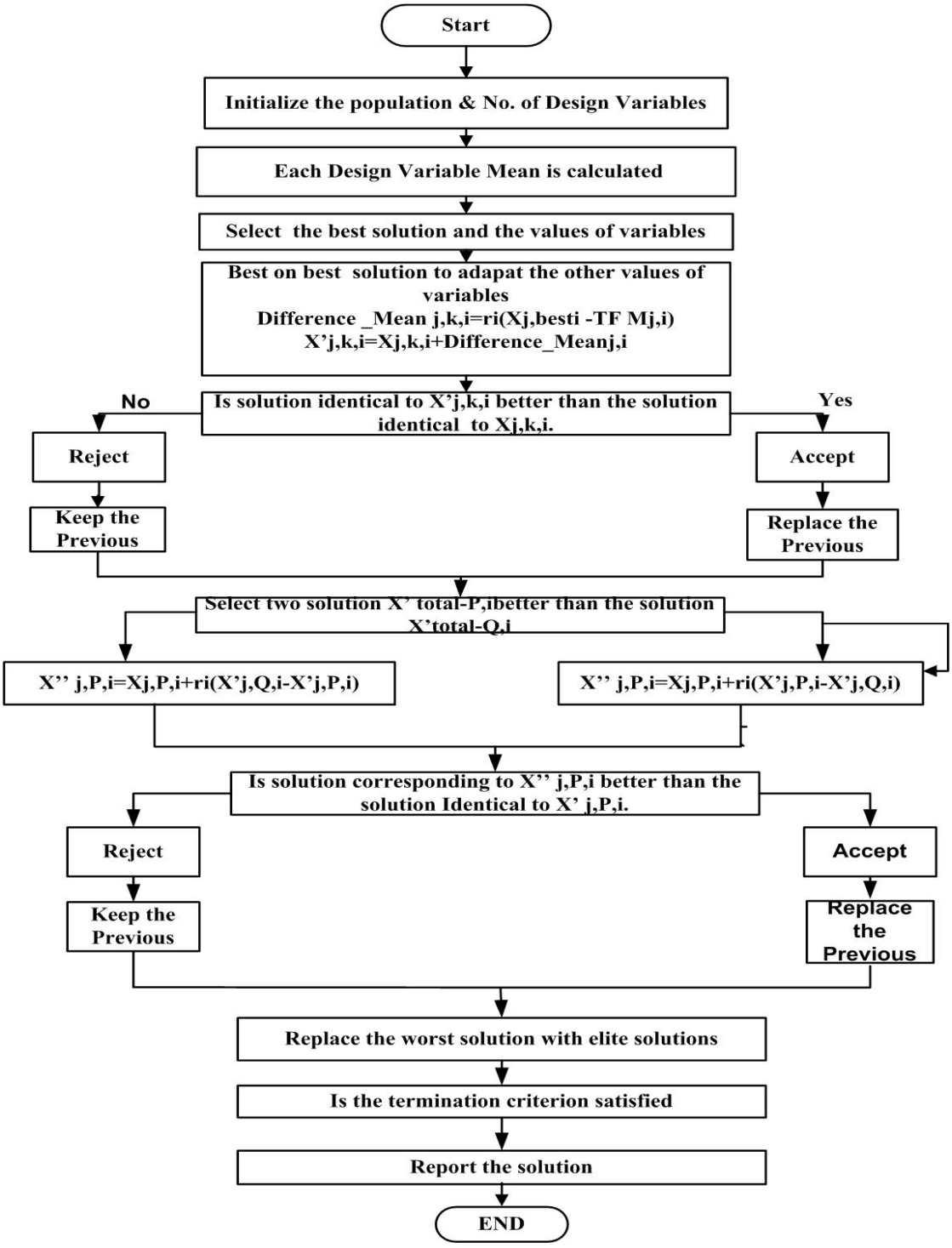

Fig. 5. Flow chart for Teaching Learning Optimization algorithm

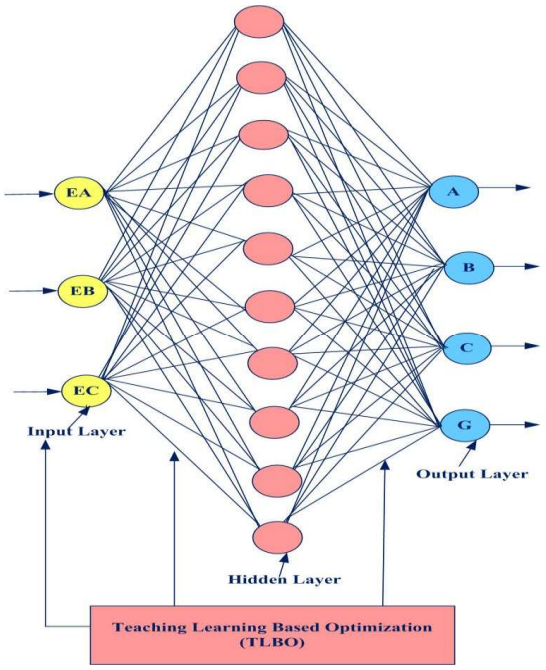

Fig. 6. Architecture of TLBO-ANN classifier

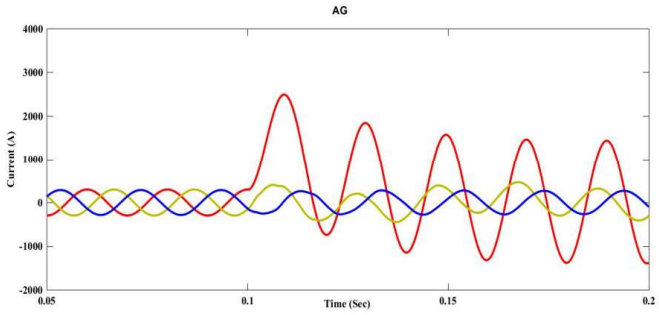

Fig. 7. Line currents waveforms during AG fault, the fault created at t=0.1sec.

are shown in Fig. 7. In this study, for demonstration purposes, an AG fault is created at t=0.1 sec and processed through EMD to extract the six IMFs for each phase, which are shown in Fig 8-Fig 10.

5.2. Neighborhood Component Analysis

The NCA is non parametric feature ranking scheme that was maximizing an objective function [30]. The weighted distance is defined as follows

$$D_W\left(x_i, x_j\right) = \sum_{m=1}^{n} {W_m}^2 \left|x_{im} - x_{jm}\right| \tag{20}$$

where w_m is the m^{th}feature's assigned weight. The probability P_{ij} in terms of the weighted distance D_w is defined as follows

$$P_{ij} = \frac{k\left(D_w\left(x_i, x_j\right)\right)}{\sum_{j=1, j\sim i}^{n} k\left(D_w\left(x_i, x_j\right)\right)} \tag{21}$$

where k is the kernel function.

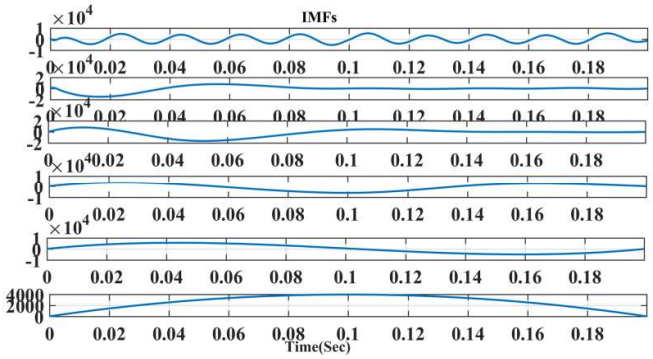

Fig. 8. The IMFs variation of phase A of the AG fault at t=0.1 sec. It consists of the 6 IMFs of the Phase A current. It can be observed that higher order IMFs contain lower frequency components than lower order IMFs.

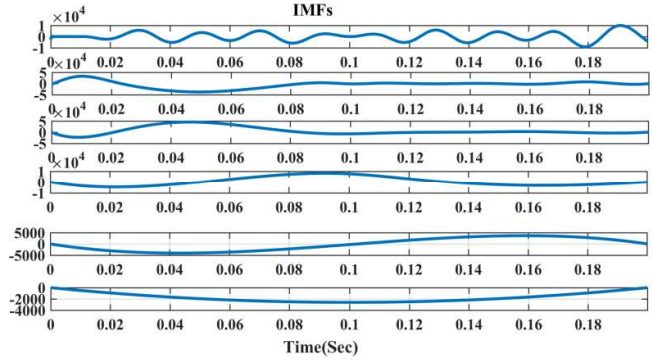

Fig. 9. The IMFs variation of phase B of the AG fault at t=0.1 sec. It consists of the 6 IMFs of the Phase A current. It can be observed that higher order IMFs contain lower frequency components than lower order IMFs.

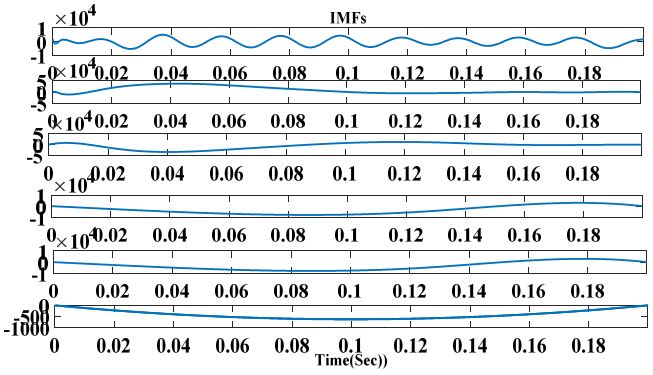

Fig. 10. The IMFs variation of phase C of the AG fault at t= 0.1 sec. It consists of the 6 IMFs of the Phase A current. It can be observed that higher order IMFs contain lower frequency components than lower order IMFs.

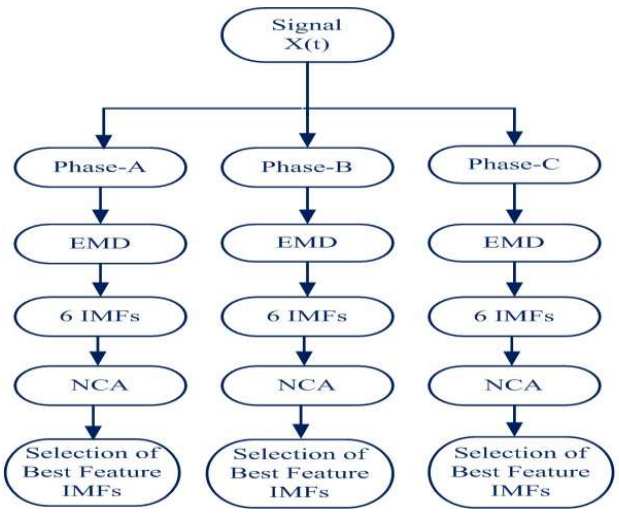

Fig. 11. Best feature IMFs identification schematic diagram

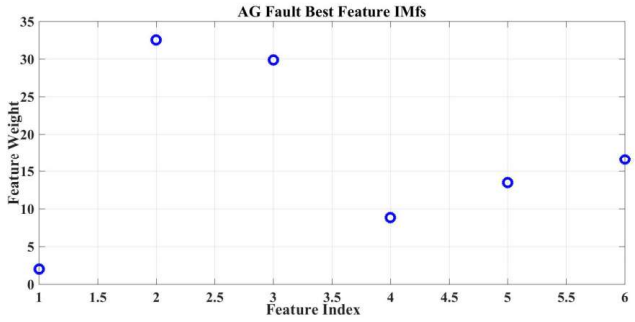

Fig. 12. Best feature selection of IMFs for AG fault

The probability of correctly classifying x_i can now be written as

$$P_i = \sum_{j=1, j\neq i}^{n} P_{ij} Y_{ij} \tag{22}$$

The $Y_i = Y_j$ does Y_{ij} indicate one.

5.3. Selection of best feature IMFs

Each phase current signal is passed through the EMD and decomposed into six IMFs. The best features are identified by applying the NCA to the six IMFs. Fig. 11 depicts the entire process.

For each fault type, the EMD extracts the six IMFs, and these IMFs data sets fit the NCA method defined by Eq.(21), the best features are selected from the higher feature weight values. For demonstration purpose, the best IMFs features for various fault are shown in Fig 12 to Fig 14 below.

The IMF's (Feature Index) with the highest degree of feature weight is considered the best feature. From Fig 12 to Fig 14, of different fault cases, the best features are selected as IMF_2 (Feature Index2) and IMF_3 (Feature Index3). Likewise, for the remaining fault cases also the best features are IMF_2 and IMF_3.

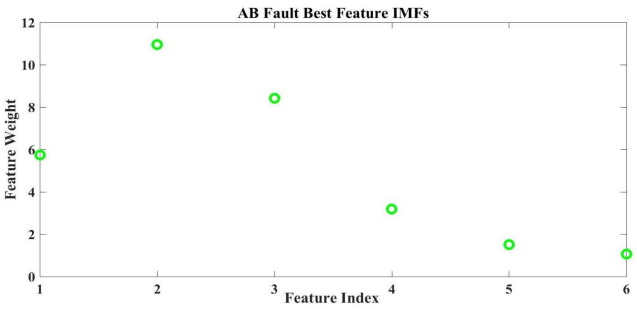

Fig. 13. Best feature selection of IMFs for AB fault

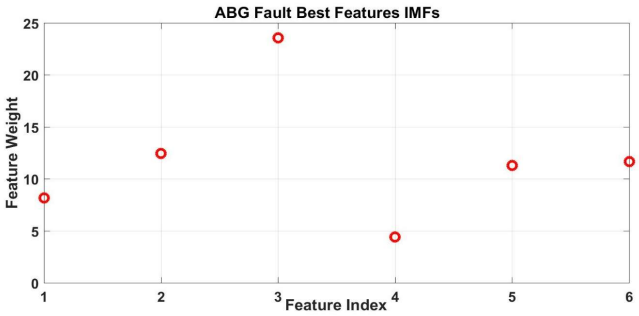

Fig. 14. Best feature selection of IMFs for ABG fault

5.4. Calculation of each phase energy

The IMF_2 and IMF_3 energy of each phase current is determined by considering the one-cycle post-fault current samples. The two energy(s) are then added to get the energy of each phase (E_A, E_B, and E_C).

The energy of each phase is calculated as follows:

Energy of phase A

$$E_A = \sum_{i=1}^{N} |IMF_2(t_1) + IMF_3(t_2)|^2 \tag{23}$$

Energy of phase B

$$E_B = \sum_{i=1}^{N} |IMF_2(t_1) + IMF_3(t_2)|^2 \tag{24}$$

Energy of phase C

$$E_C = \sum_{i=1}^{N} |IMF_2(t_1) + IMF_3(t_2)|^2 \tag{25}$$

5.5. Simulation of training and testing data for proposed intelligent classifier schemes

The extensive simulations are carried out in Fig. 1, using MATLAB simulation software to generate the training data set. The data set consists of a 18 different inception angles between 0 to 360°, 16 different locations between 0-300 km, and 17 different fault resistances between 0-200 Ω. For each fault, the totals of $18 \times 16 \times 17 = 4896$ training samples are thus generated. Table 1 displays the total training data set size for all 11 types of faults.

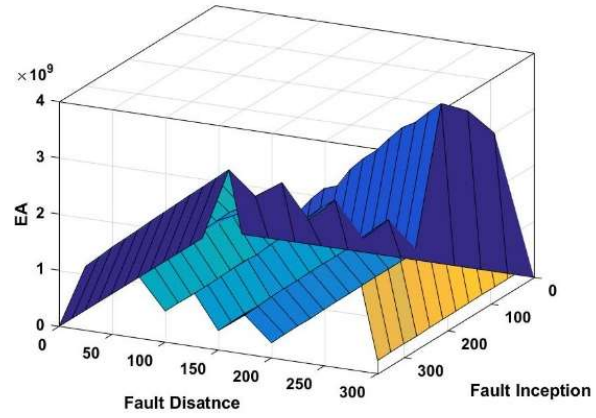

(a)

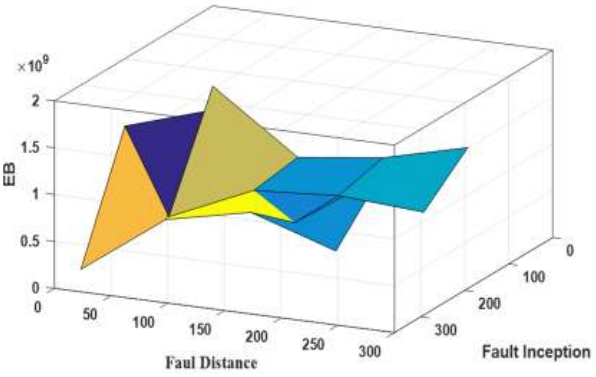

(b)

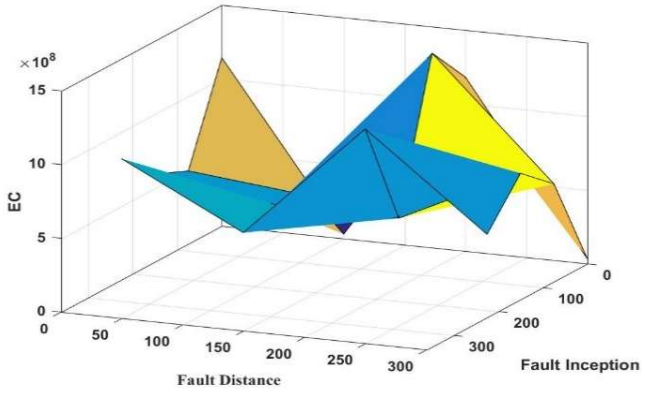

(c)

Fig. 15. Variation of phase energy(s) for various distances and fault inception angles values during AG fault a. E_A b. E_B c. E_C

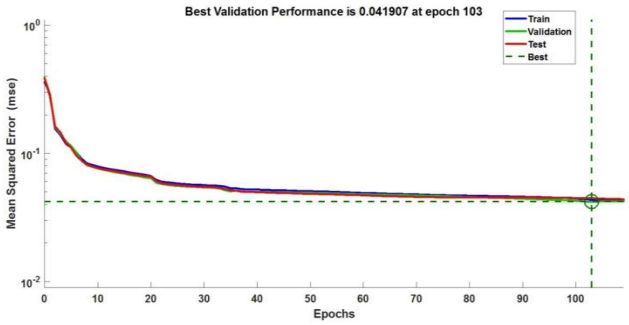

Fig. 16. Convergence characteristics of PSO-ANN classifier

The phase energy E_A, E_B, and E_C of all types of faults, training data set samples are normalized and fed as input to proposed two classifier schemes with associate targets as shown in Fig. 1. For the PSO-ANN and TLBO-ANN classifier schemes, each input sample updates the optimized weights through the respective algorithm during the network training process. In each iteration, the error is determined between the output and the target. This algorithm is repeated until it covers all training input samples and is terminated after achieving a specified Mean square error value. The Mean square error is calculated as follows.

$$MSE = \frac{1}{N}\sum_{l=1}^{n}\sum_{k=1}^{p}(y_{kl} - Y_{kl})^2 \tag{26}$$

Here the N represents the number of training samples, y_{kl} represent the target output and Y_{kl} represent the actual output. For both classier schemes, the MSE is an objective function that needs to be minimized during training and testing operations.

Finally, the proposed protection classifier schemes enable the classifier unit and it intern to enable the control unit and issue trip signal to associate circuit breaker CB as shown in Fig. 1.

6. Simulation Results, Discussions of Proposed Intelligent Classifier Schemes and Performance Indices Analysis

6.1. PSO-ANN classifier scheme test results

Fig. 1 demonstrates the proposed PSO-ANN classifier relaying scheme. The Table 2 gives the parameters of the PSO algorithm.

From Table 1, the total training samples (53856) are used to train the proposed PSO-ANN classifier, and testing samples (19008) are used to test the proposed PSO-ANN classifier. 15% of training data is used to validate the proposed classifier. Finally, the PSO terminates whenever the g_{best} values should be less than a predefined value and reached the maximum iteration.

A) Test results of PSO-ANN based classifier scheme with fault location before and after series capacitor

The number of faults properly identified among the total number of faults is known as the classification accuracy of

Table 1. Parameters for creating the data set

Parameters	Training data set	Testing data set
Types of fault	All 11 types of faults and no-fault cases	All 11 types of faults and no-fault cases
Fault resistance in Ω	$1.12, 24, \ldots, 200$ with increment of 12.	$5, 30, 60, 100, 160$ and 200
Fault inception angle in [0]	$0, 20, 40, \ldots 340°$ with increment of 20.	$10, 25, 50, 100, 150, 210, 260$ and $335°$
Fault location before and after series capacitor [km].	$12, 30, 48, \ldots, 282$ with increment of 18.	$25, 50, 75, \ldots, 275$ with increment of 25.
Compensation level [%].	40%	25%, 50% and 75%
Total patterns	$11 \times 17 \times 18 \times 16 = 53856$.	$11 \times 6 \times 8 \times 12 \times 3 = 19008$.

Table 2. PSO parameter values

PSO- Parameters	W	C1	C2	No of particles(s)	PopulationSize	No of iterations
PSO- Parameters values	Between 0.1 to rand*0.45	1.5	2.5	70	200	150

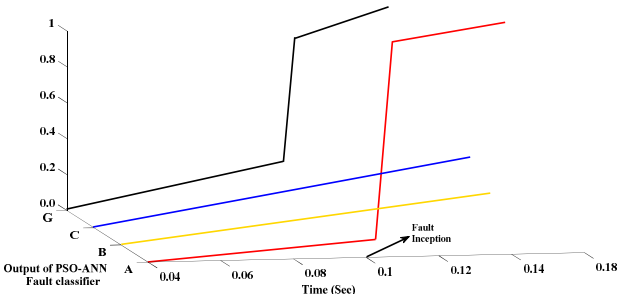

Fig. 17. PSO-ANN classifier output in time domain during AG fault at $25km$ from sending end with fault resistance 5 Ω, at t=0.1 sec.

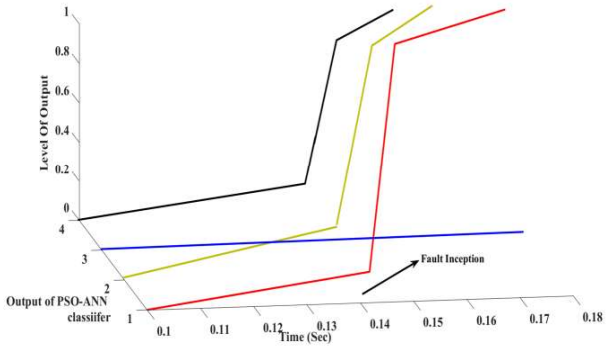

Fig. 18. PSO-ANN classifier output in time domain during AG fault at $25km$ from sending end with fault resistance 5 Ω, at t=0.1 sec.

classifier, and is expressed by Eq. (27).

$$Classification\ Accuracy\ (CA) = \frac{\text{number of accurately classified faults}}{\text{Total number of faults}} \times 100\% \quad (27)$$

From Table 3, it is observed that the fault classification time in (T_1) ms of the proposed PSO-ANN method is less than a half cycle for fault case tested.

The AG fault is created at 0.1 sec with a fault distance of 25 km from the sending end on series capacitor compensated line with fault resiatnce is 5 Ω. Fig. 17 indicates that the PSO-ANN classifier has to effectively classify the fault with less than one cycle (4 ms).

The ABG fault is created at t=0.14 sec with a fault distance of 200 km from the sending end (i.e., after series capacitor) on series capacitor compensated line with fault resistance is 30 Ω. Fig.18 indicates that the PSO-ANN classifier has to rapidly classify the fault with less than one cycle(6 ms).

PSO-ANN classifier output in time domain during ABG fault at 200 km from sending end with fault resistance 30 Ω ,at t=0.14 sec.

The confusion matrix of the PSO-ANN classifier scheme is shown in Table 4.

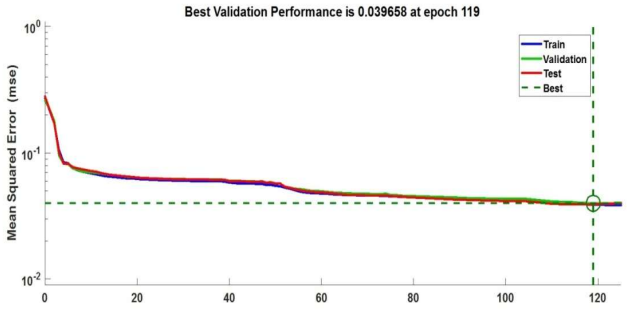

Fig. 19. Convergence characteristics of TLBO-ANN classifier

6.2. TLBO-ANN classifier scheme test results

The proposed TLBO-ANN classifier relaying scheme is shown in Fig. 1. The Table 5 gives the parameters of the TLBO algorithm.

From Fig. 16 and Fig. 19 it is observed that, the TLBO-ANN classifier scheme is achieved better convergence characteristics and improved accuracy as compared to PSO-ANN classifier.

When the fault occurs on the transmission line, the fault detection unit is activated first, and then it activates the classification unit. From Table 1, the total training samples

Table 3. Sample test results of PSO-ANN based classifier scheme

Fault Type	Fault location in km		Fault resistance in Ω	Fault inception angle ($^\circ$)	Fault classification time (T_1) (ms)	Output of PSO-ANN			
						A	B	C	G
AG	Before Series Capacitor	25	5	10	4	1	0	0	1
ABG		50	30	25	5	1	1	0	1
AB		75	100	100	8	1	1	0	0
ABC		125	60	210	7	1	1	1	0
AG	After Series Capacitor	175	100	50	8	1	0	0	1
ABG		200	30	100	6	1	1	0	1
AB		225	160	260	8	1	1	0	0
ABC		275	200	335	9	1	1	1	0

Table 4. Confusion matrix and percentage accuracy of proposed PSO-ANN classifier scheme for all 11 types of faults

Fault	1	2	3	4	5	6	7	8	9	10	11	Proposed PSO-ANN %Accuracy
1	**1**	0	0	0	0	0	0	0	0	0	0	100%
2	0	**1**	0	0	0	0	0	0	0	0	0	100%
3	0	0	**0**	0	**4**	0	0	0	0	0	0	99.91%
4	0	0	0	**0**	0	0	**2**	**2**	0	0	0	99.91%
5	0	0	**0**	0	**0**	0	**2**	**4**	0	0	0	99.87%
6	0	0	**5**	0	0	**0**	0	0	0	0	0	99.89%
7	0	0	0	**3**	0	0	**0**	0	0	0	0	99.93%
8	0	0	0	0	**4**	0	0	**0**	0	0	0	99.91%
9	0	0	0	0	0	0	0	0	**1**	0	0	100%
10	0	0	0	**6**	0	0	0	0	0	**0**	0	99.87%
11	0	0	0	0	0	**5**	0	0	0	0	**0**	99.89%
Overall classification accuracy												99.92%

Table 5. TLBO-Common parameters values

TLBO-common parameters	Population Size	Number of generations
TLBO-common parameters values	200	150

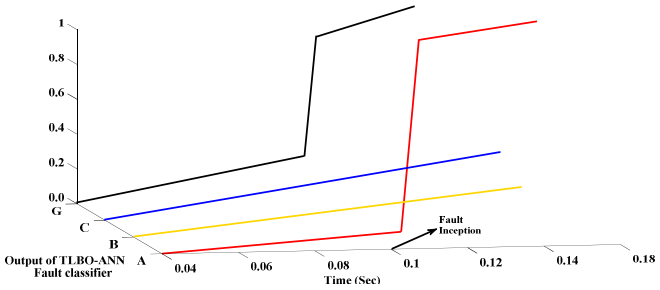

Fig. 20. TLBO-ANN based classifier output in time domain during AG fault at 50 km from sending end with fault resistance 5 Ω ,at t=0.1 sec.

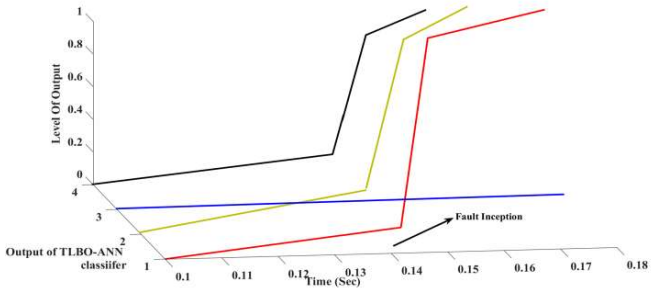

Fig. 21. TLBO-ANN based classifier output in time domain during ABG fault at 225 km from sending end with fault resistance 60 Ω ,at t=0.14 sec.

(53856) are used to train the proposed TLBO-ANN network, and the total testing samples (19008) are used to test the TLBO-ANN network. The 15% training data set is used to validate the proposed classifier.

A) Test results of TLBO-ANN based classifier scheme with fault location before and after series capacitor

The number of faults properly recognized among the total number of faults is known as the classification accuracy of classifier, and is expressed by Eq. (27).

From Table 6, it observed that, the fault classification time in ms (T_1) of the proposed TLBO-ANN method is less than a half cycle for all fault cases tested.

The AG fault is created 50 km from the sending end at t = 0.1 sec on series capacitor compensated line with fault resistance is 5 Ω. Fig. 20 indicates that the TLBO-ANN classifier has to effectively classify the fault with less than one cycle (4ms).

The ABG fault is created at t=0.14 sec with a fault distance of 225 km from the sending end (i.e., after series capacitor) on series capacitor compensated line with fault resistance is 60 Ω. Fig. 21 indicates that the TLBO-ANN classifier has to rapidly classify the fault with less than one cycle (6ms).

The confusion matrix of the TLBO-ANN classifier scheme is shown in Table 7.

6.3. Performance Analysis of Proposed Classifiers

From Fig. 22, the kappa statistic (KS) for the PSO-ANN classifier is 0.995, and for the TLBO-ANN classifier, it was improved to 0.998, suggesting that the classifier is accurate

Table 6. Sample test results of TLBO-ANN classifier scheme

Fault Type	Fault location in km	Fault resistance in Ω	Fault inception angle ($^\circ$)	Fault classification time (T_1) (ms)	Output of TLBO-ANN classifier scheme			
					A	B	C	G
AG	Before Series Capacitor	25	100	25	6	1	0	0	1
ABG		50	5	100	4	1	1	0	1
AB		75	60	150	6	1	1	0	0
ABC		125	160	210	7	1	1	1	0
AG	After Series Capacitor	175	100	25	4	1	0	0	1
ABG		200	30	50	4	1	1	0	1
AB		225	60	335	6	1	1	0	0
ABC		275	200	260	9	1	1	1	0

Table 7. Confusion matrix and percentage accuracy of proposed TLBO-ANN classifier scheme for all 11 types of faults

Fault	1	2	3	4	5	6	7	8	9	10	11	Proposed TLBO-ANN %Accuracy
1	**1**	0	0	0	0	0	0	0	0	0	0	100%
2	**0**	**1**	0	0	0	0	0	0	0	0	0	100%
3	0	0	**1**	0	0	0	0	0	0	0	0	100%
4	0	0	0	**0**	0	0	0	**2**	0	0	0	99.95%
5	0	0	0	0	**0**	0	0	0	0	0	**2**	99.95%
6	0	0	0	0	0	**0**	0	0	0	**1**	0	99.97%
7	0	0	0	0	0	0	**1**	0	0	0	0	100%
8	0	0	0	0	0	0	0	**1**	0	0	0	100%
9	0	0	0	0	0	0	0	0	**1**	0	0	100%
10	0	0	0	**2**	0	0	0	0	0	**0**	0	99.95%
11	0	0	0	0	0	**1**	0	0	0	0	**0**	99.97%
Overall classification accuracy												99.98%

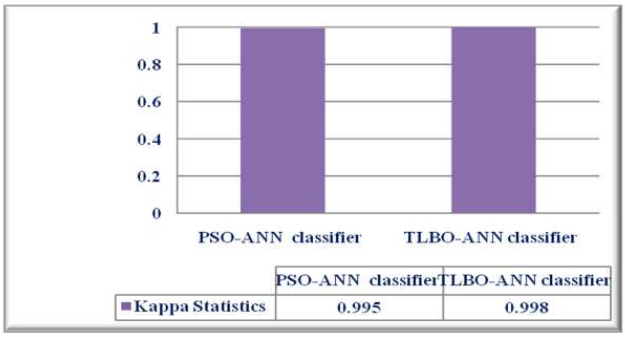

Fig. 22. Kappa statistics of PSO-ANN and TLBO-ANN classifiers

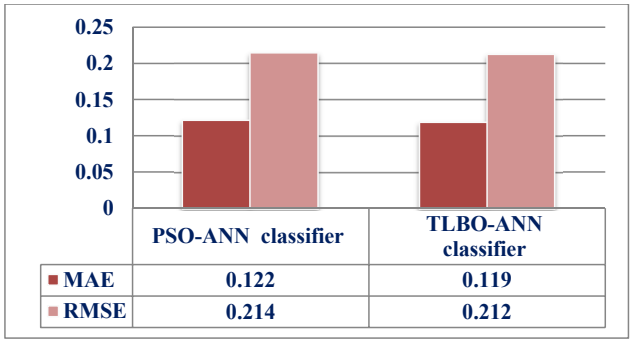

Fig. 23. MAE and RMSE statistics of PSO-ANN and TLBO-ANN classifiers

and robust. From Fig. 23, the PSO-ANN classifiers MAE (0.122) and RMSE (0.214) and MAE (0.119) and RMSE (0.212) of the TLBO-ANN classifier were lower than those of the PSO-ANN classifier, indicating that the classifier is superior.

From Fig. 24, the precision and recall results for PSO-ANN classifiers are 0.9/0.94 and the TLBO-ANN classifier improves it by 0.94/0.98. From Fig. 25, the F-measure and ROC result for the PSO-ANN classifier show 0.883/0.95 and TLBO-ANN classifier has been improved to a level of 0.99/0.97, higher than the PSO-ANN classifier.

From the above performance analysis evaluation, the TLBO-ANN intelligent classifier scheme is superior over PSO-ANN intelligent classifier scheme in terms of classification accuracy and indices efficiency.

7. Evolution of Case Studies and Comparative Assessment with Different Existing Methods

7.1. Performance during variation in load angle of generator with capacitor switching

The $20\,MVR$ capacitor load is switched at Bus-2 of Fig.1.creates the switching transients in the current waveform. With the variation of generator load angle of 10°, and 20° the capacitor switching transients are generated as shown in Fig 26–Fig 27 and tested with proposed intelligent classifier schemes.

The proposed scheme's efficiency is also tested against

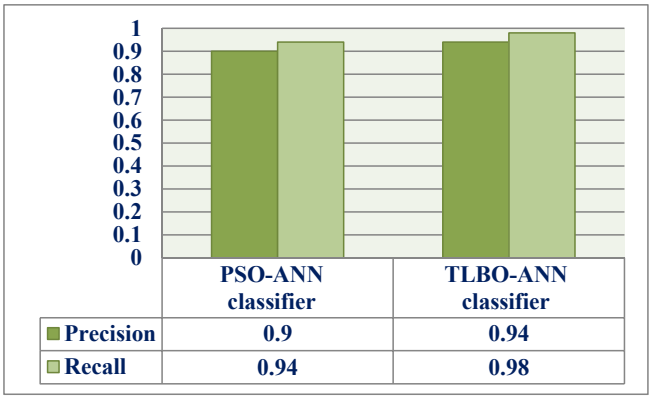

Fig. 24. Precision and Recall statistics of PSO-ANN and TLBO-ANN classifiers

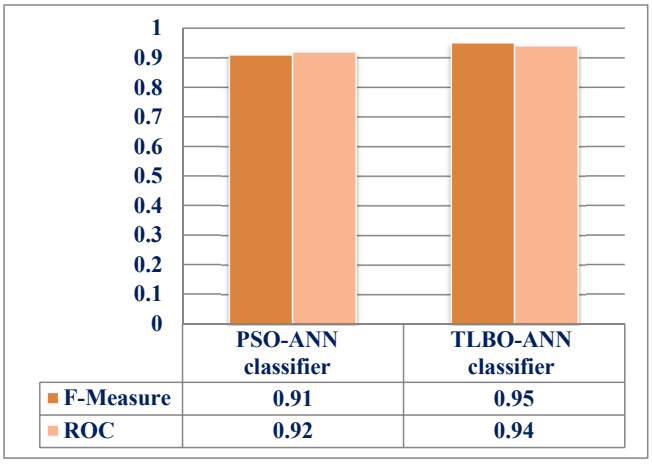

Fig. 25. F-Measure and ROC statistics of PSO-ANN and TLBO-ANN classifiers

different load angles, such as 10° ,20° and 30°. Table 9 and Table 10 show the outcomes of the tests. The proposed schemes are robust to variations in the load angles.

7.2. Performance during changing the compensation level of series capacitor

The proposed classifiers scheme's efficiency is also tested against various compensation levels, such as 10%, 25%, 50%, and 75%. The results of the tests are shown in Tables 11 and Table 12. The proposed schemes are resistant to an extensive range of compensation levels.

Table 8. Loading condition of the system

Location	BUS-2
Loading	10 MW +20 MVR
Generator load angles	10° ,20° and 30°

7.3. Performance during the power fluctuations

Due to continues load variations on series capacitor compensation transmission line the power fluctuations occur. This effect on proposed methods is evaluated in Table 13 and 14.

7.4. Performance during the load connection and disconnection

Due to sudden load injection and load dispatch happen on the series capacitor compensated line. This effect on proposed methods is evaluated in Table 15 and 16.

7.5. Performance during the change of line parameters

Due to aging and environmental conditions on series capacitor compensated line. The line parameters like resistance and inductance are changes. This effect on proposed methods is evaluated in Table 17 and 18.

7.6. Performance during the change in the operation mode of the series capacitor

Due to series capacitor compensation the interaction of the reactance of series capacitor and 300 km transmission line distributed parameters will result in mode (Hz) is occur. This effect on proposed methods is evaluated in Table 19 and 20.

Similarly, for the remaining fault cases, the corresponding mode(Hz) is show in Table 19.

7.7. Performance during the noisy conditions

To validate the efficacy of the proposed methods, the different noisy test data sets with the SNR of 20, 30, and 40 dB is considered. Few test outcomes are listed in Table 21 and 22 that represents the performance of the proposed methods under distinct noisy environment.

7.8. Comparative assessment of the proposed classifiers with different existing methods

From Table 4, the fault classification success accuracy of the proposed PSO-ANN classifier method ranges from 99.87% to 100%, with 99.92% average percentage success along with all operating conditions of the system. Similarly, from Table 7, the fault classification success accuracy of the proposed TLBO-ANN classifier ranges from 99.95% to 100%, with an average percentage success of 99.98% along with all operating conditions of the system. Compared to existing techniques, the advantage of the proposed classifier schemes is that the input features are 3. The sampling frequency is 8 kHz, is selected for one cycle post fault samples, and fault classification response time is less than a half cycle. Table 23 reveals that all existing approaches for fault classification use the signal processing method for feature extraction but in proposed methods of classification use the advanced signal processing and NCA method for feature extraction. Furthermore, the performance indices are evaluated on proposed classifiers. Compared to all existing methods, the proposed classifier methods obtained the high percentage success accuracy for the classification of faults in the series capacitor compensated transmission line.

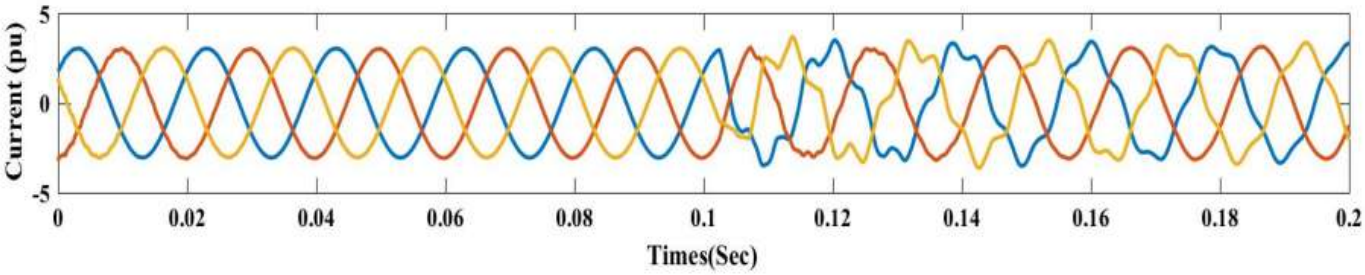

Fig. 26. Three current waveform for 10 MW active load switching and 20 MVR capacitive load switching at bus-2 with 10° generator load angle switching.

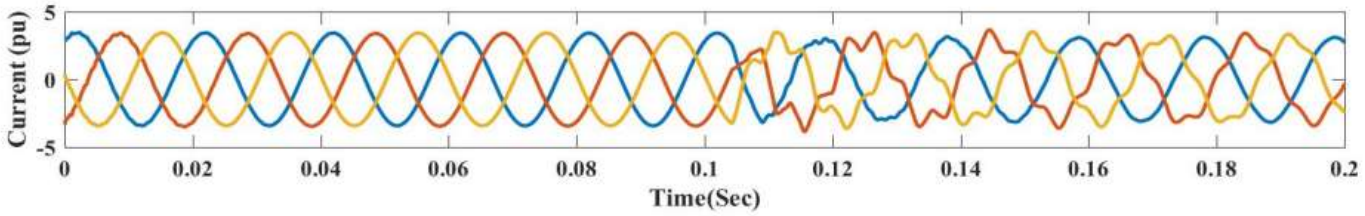

Fig. 27. Three phase current waveform for 10 MW active load switching and 20 MW capacitive load switching at bus-2 with 20° generator load angle switching.

Table 9. The performance during variation in load angles for PSO-ANN classifier

Load angles	**Fault Type**	**Fault location in (km)**	**Fault resistance in (Ω)**	**Fault inception angle ($^\circ$)**	**Fault classification time (T_1) in (ms)**	**Output of PSO-ANN classifier**
10°	AG	25	5	10	4	AG
	ABG	150	160	50	8	ABG
	AB	50	60	25	5	AB
	ABC	225	100	150	9	ABC
20°	BG	25	5	210	3	BG
	BCG	175	60	260	5	BCG
	BC	100	30	100	4	BC
	ABC	250	160	210	9	ABC
30°	CG	50	5	335	3	CG
	CAG	75	100	150	6	CAG
	CA	125	60	25	4	CA
	ABC	250	200	260	9	ABC

Table 10. The performance during variation in load angles for TLBO-ANN classifier

Load angles	**Fault Type**	**Fault location in (km)**	**Fault resistance in (Ω)**	**Fault inception angle ($^\circ$)**	**Fault classification time (T_1) in (ms)**	**Output of TLBO-ANN classifier**
10°	AG	50	5	25	4	AG
	ABG	100	30	10	6	ABG
	AB	25	100	150	7	AB
	ABC	225	160	100	9	ABC
20°	BG	25	5	210	3	BG
	BCG	175	60	335	5	BCG
	BC	100	30	260	4	BC
	ABC	250	160	50	9	ABC
30°	CG	25	5	25	3	CG
	CAG	75	160	335	7	CAG
	CA	150	30	260	4	CA
	ABC	225	200	160	9	ABC

Table 11. Performance during variation of compensation level for PSO-ANN classifier

X_c(%)	Fault Type	Fault location in (km)	Fault resistance in (Ω)	Fault inception angle ($^\circ$)	Fault classification time (T_1) in (ms)	Output of PSO-ANN classifier
10%	AG	30	30	30	4	AG
	ABG	180	160	60	6	ABG
	AB	80	60	120	8	AB
	ABC	270	200	240	9	ABC
25%	AG	25	30	25	4	AG
	ABG	175	160	50	8	ABG
	AB	75	60	100	7	AB
	ABC	250	200	210	9	ABC
50%	BG	25	5	335	3	BG
	BCG	150	60	150	5	BCG
	BC	100	100	10	8	BC
	ABC	225	160	25	9	ABC
75%	CG	50	5	335	3	CG
	CAG	75	60	260	6	CAG
	CA	125	160	100	9	CA
	ABC	250	100	210	8	ABC

Table 12. Performance during variation of compensation level for TLBO-ANN classifier

X_c(%)	Fault Type	Fault location in (km)	Fault resistance in (Ω)	Fault inception angle ($^\circ$)	Fault classification time (T_1) in (ms)	Output of TLBO-ANN classifier
10%	BG	20	10	320	8	BG
	BCG	150	50	180	4	BCG
	BC	60	120	30	5	BC
	ABC	250	180	60	6	ABC
25%	AG	25	30	10	4	AG
	ABG	175	160	50	8	ABG
	AB	75	60	100	5	AB
	ABC	250	200	210	9	ABC
50%	BG	25	5	150	3	BG
	BCG	150	60	335	6	BCG
	BC	100	100	260	8	BC
	ABC	225	160	10	9	ABC
75%	CG	50	5	25	3	CG
	CAG	75	60	50	6	CAG
	CA	125	160	210	9	CA
	ABC	250	100	260	8	ABC

Table 13. Performance during power fluctuations for PSO-ANN classifier

Power Variations 20 MW (%)	Fault Type	Fault location in (km)	Fault resistance in (Ω)	Fault inception angle ($^\circ$)	Fault classification time (T_1) in (ms)	Output of PSO-ANN classifier
30	AG	60	10	10	4	AG
	ABG	75	80	40	5	ABG
	AB	100	30	140	7	AB
	ABC	180	140	220	6	ABC
30	AG	75	20	240	5	AG
	ACG	120	80	160	4	ACG
	AC	180	100	40	6	AC
	ABC	240	150	80	7	ABC

Table 14. Performance during power fluctuations for TLBO-ANN classifier

Power Variations 20 MW (%)	**Fault Type**	**Fault location in (km)**	**Fault resistance in (Ω)**	**Fault inception angle ($^\circ$)**	**Fault classification time (T_1) in (ms)**	**Output of TLBO-ANN classifier**
30	AG	80	10	30	5	AG
	ABG	100	50	60	4	ABG
	AB	150	40	120	6	AB
	ABC	230	140	200	7	ABC
30	AG	100	30	220	6	AG
	ACG	50	50	180	5	ACG
	AC	150	120	30	4	AC
	ABC	270	180	60	7	ABC

Table 15. Performance during load connection and disconnection for PSO-ANN classifier

Load 10 MW and 20 MVR at Bus2	**Fault Type**	**Fault location in (km)**	**Fault resistance in (Ω)**	**Fault inception angle ($^\circ$)**	**Fault classification time (T_1) in (ms)**	**Output of PSO-ANN classifier**
Load Connection	AG	50	20	30	7	AG
	ABG	100	100	60	5	ABG
	AB	180	50	120	6	AB
	ABC	230	160	200	8	ABC
Load Disconnection	AG	60	30	260	7	AG
	ACG	150	60	140	4	ACG
	AC	90	120	30	6	AC
	ABC	270	170	60	5	ABC

Table 16. Performance during load connection and disconnection for TLBO-ANN classifier

Load 10 MW and 20 MVR at Bus2	**Fault Type**	**Fault location in (km)**	**Fault resistance in (Ω)**	**Fault inception angle ($^\circ$)**	**Fault classification time (T_1) in (ms)**	**Output of TLBO-ANN classifier**
Load Connection	AG	60	10	10	6	AG
	ABG	120	120	80	4	ABG
	AB	180	40	100	5	AB
	ABC	250	140	220	7	ABC
Load Disconnection	AG	75	20	240	6	AG
	ACG	180	40	120	4	ACG
	AC	100	140	40	5	AC
	ABC	240	180	80	7	ABC

Table 17. Performance during change of line parameters for PSO-ANN classifier

Change in line parameter (%)	**Fault Type**	**Fault location in (km)**	**Fault resistance in (Ω)**	**Fault inception angle ($^\circ$)**	**Fault classification time (T_1) in (ms)**	**Output of PSO-ANN classifier**
+10	AG	50	10	10	6	AG
	ABG	120	120	80	4	ABG
	AB	200	40	100	7	AB
	ABC	80	180	220	8	ABC
-10	AG	40	5	280	6	AG
	ACG	130	40	160	5	ACG
	AC	75	100	20	4	AC
	ABC	230	160	80	7	ABC

Table 18. Performance during change of line parameters for TLBO-ANN classifier

Change in line parameter (%)	Fault Type	Fault location in (km)	Fault resistance in (Ω)	Fault inception angle ($^\circ$)	Fault classification time (T_1) in (ms)	Output of TLBO-ANN classifier
+10	AG	60	5	30	6	AG
	ABG	100	100	60	5	ABG
	AB	175	30	120	4	AB
	ABC	230	140	230	7	ABC
-10	AG	75	30	60	5	AG
	ACG	150	60	140	6	ACG
	AC	30	120	40	4	AC
	ABC	200	160	100	7	ABC

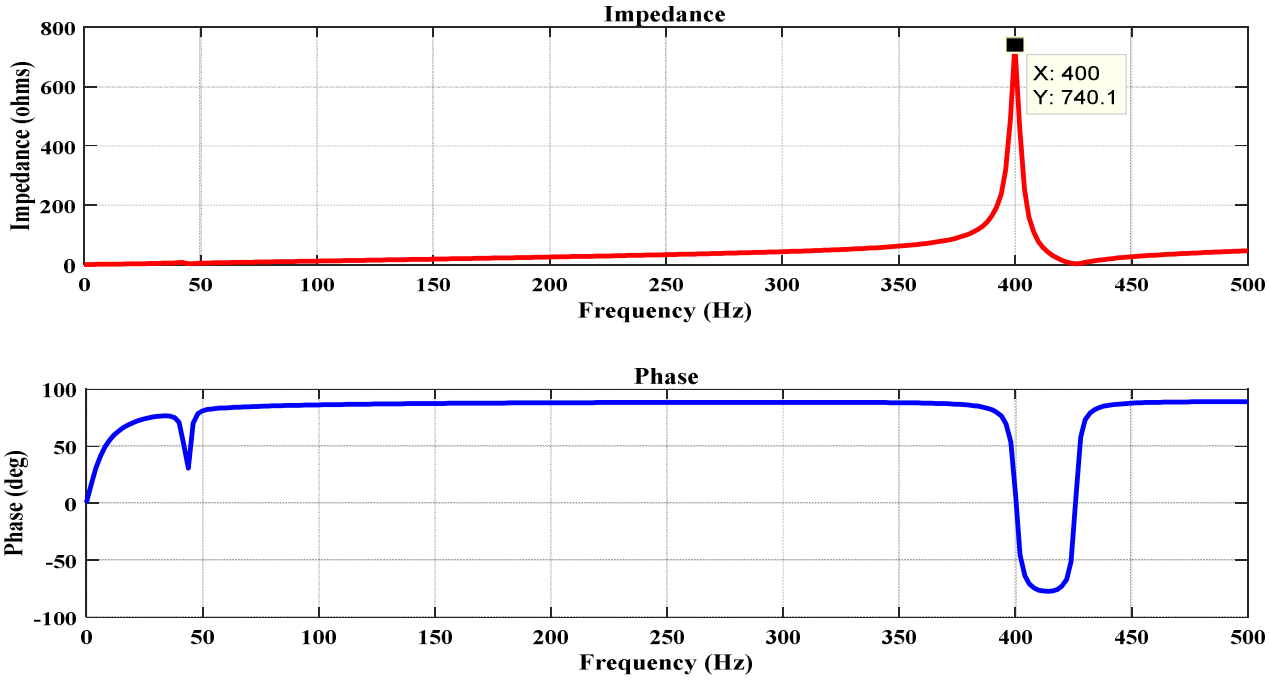

Fig. 28. Impedance measurement for AG fault occur at 30 km with fault resistance of 10 Ω and 30° deg inception angle.

Table 19. Performance during the series capacitor mode(Hz) for PSO-ANN classifier

X_c(%)	Mode(Hz)	Fault Type	Fault location in (km)	Fault resistance in (Ω)	Fault inception angle ($^\circ$)	Fault classification time (T_1) in (ms)	Output of PSO-ANN classifier
30%	400	AG	30	10	30	5	AG
	352	ABG	100	60	60	6	ABG
	424	AB	175	100	120	8	AB
	424	ABC	230	150	210	7	ABC
40%	424	BG	50	5	300	4	BG
	424	BCG	120	80	140	7	BCG
	370	BC	180	120	30	5	BC
	424	ABC	250	150	40	9	ABC
60%	424	CG	50	5	225	4	CG
	424	CAG	75	60	120	6	CAG
	424	CA	200	160	80	7	CA
	424	ABC	250	100	60	8	ABC

Table 20. Performance during the series capacitor mode(Hz) for TLBO-ANN classifier

X_c(%)	Mode(Hz)	Fault Type	Fault location in (km)	Fault resistance in (Ω)	Fault inception angle ($^\circ$)	Fault classification time (T_1) in (ms)	Output of TLBO-ANN classifier
30%	400	AG	30	10	30	4	AG
	352	ABG	100	60	60	6	ABG
	424	AB	175	100	120	8	AB
	424	ABC	230	150	210	7	ABC
40%	424	BG	50	5	300	4	BG
	424	BCG	120	80	140	6	BCG
	370	BC	180	120	30	8	BC
	424	ABC	250	150	40	9	ABC
60%	424	CG	50	5	225	5	CG
	424	CAG	75	60	120	6	CAG
	424	CA	200	160	80	8	CA
	424	ABC	250	100	60	9	ABC

Table 21. Performance during the noisy conditions for PSO-ANN classifier

SNR (dB)	Fault Type	Fault location in (km)	Fault resistance in (Ω)	Fault inception angle ($^\circ$)	Fault classification time (T_1) in (ms)	Output of PSO-ANN classifier
20	AG	40	20	20	5	AG
	ABG	200	100	40	7	ABG
	AB	75	20	140	9	AB
	ABC	250	150	220	8	ABC
30	BG	10	15	280	8	BG
	BCG	120	60	150	6	BCG
	BC	80	100	30	4	BC
	ABC	200	120	60	5	ABC
40	CG	30	30	300	7	BG
	CCG	180	80	150	8	BCG
	CC	60	110	40	4	BC
	ABC	230	150	80	5	ABC

Table 22. Performance during the noisy conditions for TLBO-ANN classifier

SNR (dB)	Fault Type	Fault location in (km)	Fault resistance in (Ω)	Fault inception angle ($^\circ$)	Fault classification time (T_1) in (ms)	Output of TLBO-ANN classifier
20	AG	50	10	30	6	AG
	ABG	175	120	60	8	ABG
	AB	100	30	120	5	AB
	ABC	200	160	230	7	ABC
30	BG	30	25	200	9	BG
	BCG	130	75	120	8	BCG
	BC	150	120	40	5	BC
	ABC	230	165	80	4	ABC
40	CG	75	10	240	6	BG
	CCG	200	70	120	9	BCG
	CC	100	120	60	7	BC
	ABC	175	160	100	4	ABC

Table 23. Comparative assessment of proposed classifier schemes with existing classifiers techniques

Ref	[3]	[4]	[5]	[8]	Proposed Classifier Schemes
Type of transmission line	Uncompensated line	Uncompensated line	Series capacitor compensated line.	Uncompensated line	Series capacitor compensated line
Signal processing technique	Wavelet transform	–	Wavelet transform	Wavelet transform	Empirical mode decomposition
Type of classifier	PSO-multilayer perceptron MLP	Decision tree	Hybrid-PSO-artificial neural network	Chebyshev neural network	PSO-ANN and TLBO-ANN
Number of input features	4	6	11	4	3
Fault classification	Yes	Yes	Yes	Yes	Yes
Number of cycles used	One cycle	One cycle	–	One cycle	One cycle
High resistance in ohm (Ω)	0-200 Ω	0-300 Ω	0-200 Ω	0 -150 Ω	0-200 Ω
Fault types	10	10	11	10	11
Fault inception angle ($\circ$)	0-360°	0-90^0	-	0-115^0	0-360^0
Fault location (km)	0- 300 km	0-290 km	0-900 km	0-300 km	0-300 km
Capacitor switching event	–	–	–	Yes	Yes
Different compensation levels	–	–	–	Yes	Yes
Load angles variations ($\circ$)	–	10° – 30°	–	10°-30°	10°-30°
Fault patterns	48,960	18,100	1,650	23,400	53,865
Percentage Accuracy	99.91%	100%	99.71%	98.56%	99.92% and 99.98%
Fault classification time	–	less than half cycle	–	less than half cycle	less than half cycle
Evolution of performance indices (PI)	–	–	–	–	Yes

"Yes" =Considered and "–"= Not mentioned.

8. Conclusions

The following conclusions are drawn from several fault simulation cases with a wide range of the system operating conditions.

- The proposed classifier schemes capturing the sending end currents, and hence it is free from synchronization errors
- The proposed classifier schemes utilize the current signals, thus voltage inversion has no impact on performance.
- The volume of memory required for feature extraction by the empirical mode decomposition and neighborhood component analysis is low because it extracted two best feature Intrinsic mode functions out of six intrinsic mode functions.
- To evaluate the energy values of each phase using the best features intrinsic mode functions is simple.
- The TLBO-ANN classifier offers superior classification accuracy 99.98% than the classification accuracy of PSO-ANN classifier 99.92%.
- From the performance indices evaluation results, the TLBO-ANN classifier is significantly superior to the PSO-ANN classifier.
- The robustness of the proposed two classifiers has been validated with capacitor switching event and different compensation level conditions.
- The proposed two classifiers have been classified the faults in rapid time, less than a half cycle.
- The efficacy of the proposed two classifier schemes is higher than the existing approaches.

References

[1] M.T. Hoq, J. Wang, and N. Taylor, "Review of recent developments in distance protection of series capacitor compensated lines," *Electr. Power Syst. Res.*, vol. 190, p. 106831, 2021.

[2] B. Vyas, R.P. Maheshwari, and B. Das, "Protection of series compensated transmission line: issues and state of art," *Electr. Power Syst. Res.*, vol. 107, pp. 93–108, 2014.

[3] E. Shehab-Eldin and P. McLaren, "Travelling wave distance protection-problem areas and solutions," *IEEE Trans. Power Deliv.*, vol. 3, no. 3, pp. 894–902, 1988.

[4] O. A. Youssef, "Combined fuzzy-logic wavelet-based fault classification technique for power system

Appendix-A

Test Power System Simulation data

Parameters	Sources	
	Sending end	**Receiving end**
Source Voltages	$500\angle 30°kV$ $Z_{s1} = 15.23 + j42.53\Omega$ $Z_{s0} = 2.15 + j12.15\Omega$	$500\angle 0°kV$ $Z_{r1} = 13.53 + j43.27\Omega$ $Z_{r0} = 0.54 + j1.19\Omega$
Transmission line		
Length of the Line 1	$150\,km$	
Length of the Line 2	$150\,km$	
Positive sequence impedance	$0.01262 + j0.2928(\Omega/km)$	
Zero sequence impedance	$0.3583 + j1.259(\Omega/km)$	
Positive sequence capacitance	$12.63(\eta F/km)$	
Zero sequence capacitance	$7.740(\eta F/km)$	
Series capacitor with 40% compensation	$90.6\mu F$	

relaying," *IEEE Trans. Power Deliv.*, vol. 19, no. 2, pp. 582–589, 2004.

[5] A.A. Girgis and M.B. Johns, "A hybrid expert system for faulted section identification, fault type classification and selection of fault location algorithms," *IEEE Power Eng. Rev.*, vol. 9, no. 4, pp. 56–57, 1989.

[6] J.-A. Jiang, C.-S. Chen, and C.-W. Liu, "A new protection scheme for fault detection, direction discrimination, classification, and location in transmission lines," *IEEE Trans. Power Deliv.*, vol. 18, no. 1, pp. 34–42, 2003.

[7] G. Purushothama, A. Narendranath, D. Thukaram, and K. Parthasarathy, "Ann applications in fault locators," *Int. J. Electr. Power Energy Syst.*, vol. 23, no. 6, pp. 491–506, 2001.

[8] G. Mulltilin, "D90 plus line distance protection system," in *Instruction manual*, 2012.

[9] J.B. Roberts and E.O. Schweitzer III, "Fault identification system for use in protective relays for power transmission lines," May 7 1996. US Patent 5,515,227.

[10] J. Upendar, C.P. Gupta, G.K. Singh, and G. Ramakrishna, "Pso and ann-based fault classification for protective relaying," *IET Gener. Transm. Distrib.*, vol. 4, no. 10, pp. 1197–1212, 2010.

[11] M.M. Taheri, H. Seyedi, and B. Mohammadi-ivatloo, "Dt-based relaying scheme for fault classification in transmission lines using modp," *IET Gener. Transm. Distrib.*, vol. 11, no. 11, pp. 2796–2804, 2017.

[12] P.D. Raval and A.S. Pandya, "A hybrid pso-ann-based fault classification system for ehv transmission lines," *IETE J. Res.*, vol. 68, no. 4, pp. 3086–3099, 2022.

[13] N.R. Babu and B.J. Mohan, "Fault classification in power systems using emd and svm," *Ain Shams Eng. J.*, vol. 8, no. 2, pp. 103–111, 2017.

[14] H. Malik and R. Sharma, "Emd and ann based intelligent fault diagnosis model for transmission line," *J. Intell. Fuzzy Syst.*, vol. 32, no. 4, pp. 3043–3050, 2017.

[15] B.Y. Vyas, R. Maheshwari, and B. Das, "Versatile relaying algorithm for detection and classification of fault on transmission line," *Electr. Power Syst. Res.*, vol. 192, p. 106913, 2021.

[16] P.K. Mishra, A. Yadav, and M. Pazoki, "A novel fault classification scheme for series capacitor compensated transmission line based on bagged tree ensemble classifier," *IEEE Access*, vol. 6, pp. 27373–27382, 2018.

[17] S. Bhasker, M. Tripathy, A. Agrawal, and A. Mishra, "Differential protection of ispst using chebyshev neural network," *J. Oper. Autom. Power Eng.*, vol. 11, no. 2, pp. 123–129, 2023.

[18] P. Venkata, V. Pandya, and A. Sant, "Data mining model based differential microgrid fault classification using svm considering voltage and current distortions," *J. Oper. Autom. Power Eng.*, vol. 11, no. 3, pp. 162–172, 2023.

[19] H. Taherian, I. Nazer, E. Razavi, S. Goldani, M. Farshad, and M. Aghaebrahimi, "Application of an improved neural network using cuckoo search algorithm in short-term electricity price forecasting under competitive power markets," *J. Oper. Autom. Power Eng.*, vol. 1, no. 2, pp. 136–146, 2007.

[20] M.O.F. Goni, M. Nahiduzzaman, M.S. Anower, M.M. Rahman, M.R. Islam, M. Ahsan, J. Haider, and M. Shahjalal, "Fast and accurate fault detection and classification in transmission lines using extreme learning machine," in *Adv. Electr. Electron. Eng.*, vol. 3, p. 100107, 2023.

[21] D. Gutierrez-Rojas, I.T. Christou, D. Dantas,

A. Narayanan, P.H. Nardelli, and Y. Yang, "Performance evaluation of machine learning for fault selection in power transmission lines," *Knowl. Inf. Syst.*, vol. 64, no. 3, pp. 859–883, 2022.

[22] M. Bhatnagar, A. Yadav, and A. Swetapadma, "Enhancing the resiliency of transmission lines using extreme gradient boosting against faults," *Electr. Power Syst. Res.*, vol. 207, p. 107850, 2022.

[23] Y. Pang, D. Yang, R. Teng, B. Zhou, and C. Xu, "A deep learning based multiple signals fusion architecture for power system fault diagnosis," *Sustain. Energy, Grids Netw.*, vol. 30, p. 100660, 2022.

[24] F.M. Shakiba, M. Shojaee, S.M. Azizi, and M. Zhou, "Generalized fault diagnosis method of transmission lines using transfer learning technique," *Neurocomputing*, vol. 500, pp. 556–566, 2022.

[25] N.E. Huang, Z. Shen, S.R. Long, M.C. Wu, H.H. Shih, Q. Zheng, N.-C. Yen, C.C. Tung, and H.H. Liu, "The empirical mode decomposition and the hilbert spectrum for nonlinear and non-stationary time series analysis," *Proc. R. Soc. A: Math. Phys. Eng. Sci.*, vol. 454, no. 1971, pp. 903–995, 1998.

[26] J. Kennedy and R. Eberhart, "Particle swarm optimization," in *Proc. Int. Jt. Conf. Neural Netw.*, vol. 4, pp. 1942–1948, IEEE, 1995.

[27] P.K. Simpson, *Artificial neural systems: foundations, paradigms, applications, and implementations*. McGraw-Hill, Inc., 1991.

[28] R.V. Rao, V.J. Savsani, and D. Vakharia, "Teaching–learning-based optimization: a novel method for constrained mechanical design optimization problems," *Comput. Aided Des.*, vol. 43, no. 3, pp. 303–315, 2011.

[29] A. Vinayagam, V. Veerasamy, P. Radhakrishnan, M. Sepperumal, and K. Ramaiyan, "An ensemble approach of classification model for detection and classification of power quality disturbances in pv integrated microgrid network," *Appl. Soft Comput.*, vol. 106, p. 107294, 2021.

[30] W. Yang, K. Wang, and W. Zuo, "Neighborhood component feature selection for high-dimensional data.," *J. Comput.*, vol. 7, no. 1, pp. 161–168, 2012.